Journal of Zhejiang University SCIENCE A
ISSN 1009-3095 (Print); ISSN 1862-1775 (Online)
www.zju.edu.cn/jzus; www.springerlink.com
E-mail: jzus@zju.edu.cn

Numerical simulation and optimization design of the EGR cooler in vehicle

Yu-qi HUANG[†1], Xiao-li YU[†‡1], Guo-dong LU[1,2]

([1]*Power Machinery and Vehicular Engineering Institute, Zhejiang University, Hangzhou 310027, China*)

([2]*Zhejiang Yinlun Machinery Co., Ltd., Tiantai 317200, China*)

[†]Email: huangyuqi@zju.edu.cn; yuxl@zju.edu.cn

Received Mar. 26, 2008; revision accepted May 22, 2008

Abstract: The EGR (exhaust gas recirculation) technique can greatly reduce the NO_x emission of diesel engines, especially when an EGR cooler is employed. Numerical simulations are applied to study the flow field and temperature distributions inside the EGR cooler. Three different models of EGR cooler are investigated, among which model A is a traditional one, and models B and C are improved by adding a helical baffle in the cooling area. In models B and C the entry directions of cooling water are different, which mostly influences the flow resistance. The results show that the improved structures not only lengthen the flow path of the cooling water, but also enhance the heat exchange rate between the cool and hot media. In conclusion we suggest that the improved structures are more powerful than the traditional one.

Key words: Exhaust gas recirculation (EGR) cooler, Computational fluid dynamics (CFD), Shell-and-tube heat exchanger, Helical baffle

doi:10.1631/jzus.A0820223 **Document code:** A **CLC number:** TK414.2+12; O357.5

INTRODUCTION

The diesel engine is widely used in modern vehicles. Unfortunately it is one of the major gas pollution sources since the toxics, such as nitrogen oxides (NO_x) and other pollutants, in its exhaust gas cause adverse health effects. It is well known that decreasing the gas temperature results in reductions in NO_x in the exhaust gases. In order to restrain the formation of pollutants, a high efficiency air cooler was developed to cool the gas of diesel engines (Grunenwald *et al*., 2001; Pantow *et al*., 2001; Stolz *et al*., 2001).

Considering its complicated and hostile working conditions, an EGR cooler must be compact with the following features: small volume, steady performance, easy to clean and durable in the high temperature and corrosive environment. Because of that, the shell-and-tube heat exchanger made of stainless steel is extensively adopted for cooling the exhaust gas before mixing with the charge in the intake system.

Much literature is available on the optimization of the shell-and-tube heat exchanger. Shell side baffles of different types have been widely used to promote heat exchange for several decades. A well designed baffle could not only improve the flow pattern but also strengthen the heat exchange effectively with less punishing pressure loss. Lutcha and Nemcansky (1990) found that in a single-tube heat exchanger, a helical baffle could force the shell side flow to approach a plug flow condition, which increased the average temperature driving force. The flow patterns induced by the baffles also made the shell side heat transfer increase significantly. Stehlík *et al*.(1994) conducted a comparative investigation of correction factors between segmental and helical baffles, and proved the superiority of helical baffles by data analysis. Peng *et al*.(2007) presented an experimental study of two shell-and-tube heat exchangers using helical and segment baffles alterna-

‡ Corresponding author

tively, the results indicating that the one with continuous helical baffles leads to nearly 10% increase in heat transfer coefficient compared to another one using conventional segmental baffles for the same shell-side pressure drop. Nasr *et al*.(2007) investigated the flow pattern of a shell-and-tube heat exchanger with helical baffles, and developed the relationship between the area, the heat transfer coefficient and pressure drop based upon the concept of a rapid design algorithm. Based on the study, the helical baffles are a proper replacement for the segmental baffles in shell-and-tube heat exchangers. They could remove many of the drawbacks of segmental baffles.

The shell-and-tube heat exchanger with helical baffles also showed significant improvement in the fouling behavior during operation. Master *et al*.(2003) demonstrated the helixchanger option in reducing the velocity-dependent fouling of heat exchangers. The helixchanger heat exchanger when applied in typical fouling services proved to be effective in reducing the fouling rates.

In conclusion, the helical baffle has several advantages: (1) improvement of shell side heat transfer; (2) less pressure drop for a given mass flow rate; (3) reduction in bypass effects in shell side; (4) decrease in fouling in shell side; (5) prevention of bundle vibration.

Due to its outstanding performance the helical baffle has been introduced into the EGR cooler recently. Past research focused on either experimentation with different geometric design or comparative analysis between measured results and evaluation. In the present research three design-models based on EGR coolers are presented. Commercial computational fluid dynamics (CFD) codes based upon the finite volume method is used to make the simulation. Then the numerical results are tabled and compared. The flowing mechanism and temperature fields inside are analyzed to explain the optimized phenomenon in the heat exchanger.

MODEL DESCRIPTION

The present EGR cooler consists of seven tubes, two clapboards and a shell, etc. (details are shown in Figs.1 and 2). The exhaust gas flow in the tube side converse to *Y*-axis and the water as cold medium are curtained off by a tube wall and clapboards. All the tubes and shells in the three models have the same size. Derived from the novel design, models B and C both have a helical baffle on the shell side. The detailed structure of the baffles are exactly the same, except for inlet and outlet sections of water flow which are vertical to the shell wall in model B but tangential in model C.

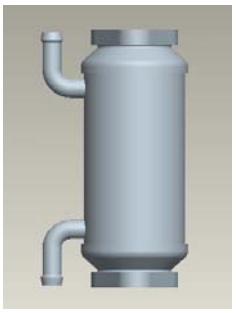

Fig.1 EGR cooler (model A and model B)

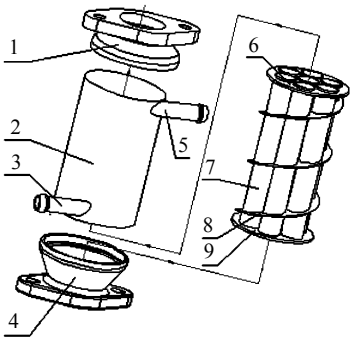

1: Gas inlet chamber; 2: Shell; 3: Water inlet section; 4: Gas outlet chamber; 5: Water outlet section; 6: Clapboard; 7: Tube; 8: Helical baffle; 9: Clapboard

Fig.2 Configuration of model C

Aiming to study the flow structure and heat exchange, a CFD program Fluent 6.3 is introduced to solve the discretized Navier-Stokes equations for heat conduction problems involved in a solid zone. The standard k-ε turbulence model with shear flow corrections is used to deal with high-speed turbulent flow problems. The second order upwind difference (UD) scheme is adopted for the momentum, energy and turbulence equations.

The standard k-ε model is a semi-empirical one, which is based on model transport equations for the turbulence kinetic energy (k) and its dissipation rate (ε). The Reynolds stresses are related to the mean

velocity gradients on the basis of the Boussinesq hypothesis. k and ε are obtained from the following transport equations:

$$\frac{\partial}{\partial t}(\rho k)+\frac{\partial}{\partial x_i}(\rho k u_i)=\frac{\partial}{\partial x_j}\left[\left(\mu+\frac{\mu_t}{\sigma_k}\right)\frac{\partial k}{\partial x_j}\right]+\rho G_k-\rho\varepsilon, \tag{1}$$

$$\frac{\partial}{\partial t}(\rho \varepsilon)+\frac{\partial}{\partial x_i}(\rho \varepsilon u_i)=\frac{\partial}{\partial x_j}\left[\left(\mu+\frac{\mu_t}{\sigma_\varepsilon}\right)\frac{\partial \varepsilon}{\partial x_j}\right]+C_{1\varepsilon}\frac{\rho\varepsilon}{k}G_k-C_{2\varepsilon}\frac{\rho\varepsilon^2}{k}. \tag{2}$$

In these equations, G_k represents the generation of turbulence kinetic energy due to the mean velocity gradients, calculated by

$$G_k=\frac{\mu_t}{\rho}\frac{\partial u_i}{\partial x_j}\left(\frac{\partial u_i}{\partial x_j}+\frac{\partial u_j}{\partial x_i}\right). \tag{3}$$

The k and ε are coupled to the governing equations via the relation

$$\mu_t=\rho C_\mu k^2/\varepsilon, \tag{4}$$

$C_{1\varepsilon}$=1.44, $C_{2\varepsilon}$=1.92, C_μ=0.09, σ_k=1.0, σ_ε=1.3.

The empirical constant for the turbulence model is assigned in accordance with the recommendation of Launder and Spalding (1972).

GRID GENERATION AND BOUNDARY CONDITIONS

The computational domain includes both the tube side and the shell side regions. Around the helical baffle in models B and C tetrahedral cells are generated, which are used in particular zones for adaptation to the complex geometrical shape. In the regions of the inlet and outlet sections, prism cells are distributed. For their accuracy and stability, the hexahedral or prism cells are preferred in the grid generation (Fig.3).

In order to establish a grid-independent solution, tests are performed. The results obtained with ten grid sizes of model A for a certain mass flow rate are shown in Fig.4, which present a pressure drop and temperature difference on the tube side at different grid sizes, corresponding to different cells numbers. It is found that the results converge at the cell number of 3615878, where the minimum size of meshes is 0.3 mm. This is to say that the simulation becomes grid independent for this size of grid; therefore all the following simulations are carried out with such a grid. It takes about 24 h for calculation on a super-computer with 6 CPUs involved. As a result, approximately 5 million mixture elements are generated for models B and C, the size of all the meshes arranged from 0.3 to 0.8 mm.

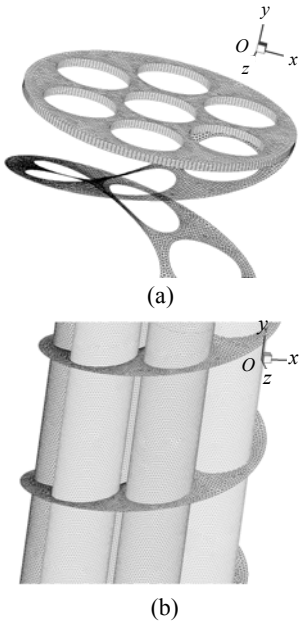

Fig.3 Computational grid of models. (a) Clapboard and helical baffle; (b) Tube and helical baffle

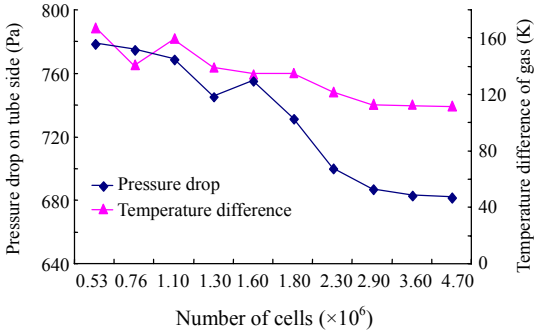

Fig.4 Pressure drop and temperature difference for different numbers of cells

In the simulation of models, boundary conditions are required for velocity, temperature and pressure. At the inlet plane of the water and gas, mass flow-rates are assumed to be constant at a particular temperature. The thickness of tube wall and helical baffle are set as zero in modeling due to their negligible size (in particular when compared to other components). On the tube and helical baffle surfaces, coupled thermal conditions are defined and shell conduction models are adopted by inputting the wall thickness correspondingly to solve the heat transfer question. Pressure outlet boundary conditions are introduced in the gas and water outlet planes.

DETERMINATION OF PERFORMANCE PARAMETERS

The pressure drop and heat transfer performance are characterized by a friction factor f and an average heat transfer coefficient h, respectively. The flow conditions can be characterized by Reynolds number. Following the conventions laid down by Dong *et al*.(2007), Re number is estimated as follows:

$$Re = \rho u d_e / \mu, \tag{5}$$

where u is the flow velocity on shell side, d_e is the hydraulic diameter of the shell side. For the models used in Dong *et al*.(2007),

$$d_e = 2(R^2 - 7r^2)/(R + 7r), \tag{6}$$

where R is the shell outside radius and r is the tube radius.

Shell side friction factor f can be written as

$$f = \frac{\Delta P}{(L/d_e)(\rho u^2/2)}. \tag{7}$$

Heat absorbed by water and supplied by hot gas, Q_c and Q_h can be written as (Eiamsa-ard and Promvonge, 2007)

$$Q_c = \dot{m}_c C_{p,c}(T_{c,out} - T_{c,in}),\ Q_h = \dot{m}_h C_{p,h}(T_{h,out} - T_{h,in}), \tag{8}$$

where $\dot{m}_c$ and $\dot{m}_h$ are the mass flow rate of water and gas, respectively; $C_{p,c}$ and $C_{p,h}$ are the specific heat of water and gas, respectively. The average heat transfer coefficient h is estimated as follows:

$$h = \overline{Q}/[A(T_b - \overline{T}_{wall})], \tag{9}$$

where

$$T_b = (T_{h,out} + T_{h,in})/2, \tag{10}$$

$$\overline{Q} = (Q_c + Q_h)/2, \tag{11}$$

$\overline{T}_{wall}$ is the average wall temperature at the outer surfaces of the tube and baffle, A is the summation of all the heat transfer areas (the helical baffle and seven tubes are included).

NUMERICAL RESULTS

In the present study five cases with different water mass flow rates are simulated. The steady state results are listed in Table 1, which exhibits the volumetric water flow, the pressure drop of shell side and the temperature contrast.

Fig.5 sketches the path lines in both water and gas flow fields. The non-arrow lines figure the path line of the gas flow in tube side converse to the Y-axis direction, which is almost the same in the three

Table 1 Simulated results of different cases

Case		Volumetric water flow (m^3/h)	ΔP of shell side (Pa)	ΔT of water (K)	ΔT of gas (K)
Model A	1	0.60	15174.25	2.85	111.88
	2	0.89	33036.29	1.94	112.31
	3	1.19	58754.17	1.46	112.65
	4	1.50	93078.26	1.16	112.96
	5	1.87	144151.76	0.93	113.27
Model B	1	0.60	17263.31	3.38	135.26
	2	0.89	37553.57	2.39	137.72
	3	1.19	67531.79	1.80	138.57
	4	1.50	105913.40	1.45	139.02
	5	1.87	163687.33	1.15	139.52
Model C	1	0.60	12944.00	3.27	130.75
	2	0.89	28096.19	2.30	131.86
	3	1.19	49803.91	1.74	132.50
	4	1.50	80038.90	1.38	133.32
	5	1.87	125286.22	1.10	133.88

ΔP: pressure difference; ΔT: temperature difference

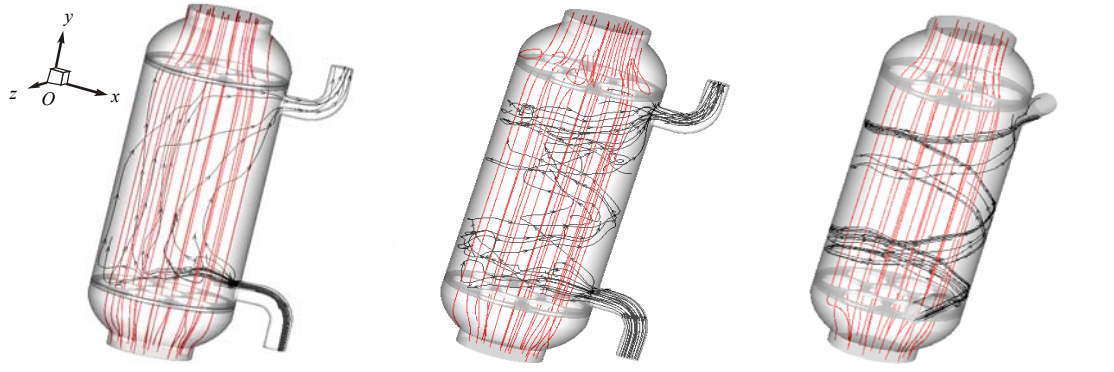

(a) (b) (c)

Fig.5 Path lines of various models ($\dot{m}_h$ = 0.89 m^3/h). (a) Model A; (b) Model B; (c) Model C

models. The arrow lines show the streamline pattern of the water. These figures show that the water flow fields are greatly inflected by using the helical baffle, which extends the flow distance and strengthens the circle flow accordingly. The shell side flow in model B is more disorganized than that in model C, which demonstrates that the tangential water-inlet design can adjust the flow pattern and decrease the turbulence intensity effectively.

Fig.6 shows velocity vectors on *X*-*Z* plane (exactly in the middle of cooler) under the condition of $\dot{m}_h$=1.5 m^3/h. All the vectors are displayed to the same scale. As seen in Fig.6a, the short vectors indicate that most of the velocity vectors are upright to *X*-*Z* plane in model A. In Figs.6b and 6c, the flows along the helical baffles are accompanied by rotation, secondary flows are generated and the flow runs parallel to the *X*-*Z* plane. The temperature distribution and path lines in part of *X*-*Z* section (model B) are shown in Fig.7. This figure illustrates the generation of a vortex. According to the field synergy principle (Guo *et al*., 1998), the overall heat exchange efficiency of the cooler is influenced by the synergy between the flow orientation and the field temperature gradients. As shown in Fig.7, the flow and temperature fields match fairly well. Basically the temperature gradients are vertical to the tube wall in these cases. A function of the helical baffle is to coordinate the flow and temperature fields to satisfy the field synergy principle. It also accounts for the distinct enhancement of heat transfer efficiency.

The temperature and heat transfer coefficient in the helical baffle are observed to be much lower than that in the tube surface (Fig.8). These figures suggest that the primary function of the helical baffle is neither to strengthen the heat exchange in itself nor to widen the diathermanous surface, but to enhance the total efficiency of heat exchange by improving the flow pattern. Because of the oriented effect of the helical baffle, the flow intensity is weakened in some particular region, which makes the temperature distribution asymmetric. Misdistributions of flow and temperature caused by the helical baffle can have a bad effect on cooler performance and reliability. Modifying the intake angle and position is an alternative approach to dealing with this problem. Anyway, the heat exchange of the whole cooler increased by using the helical baffle.

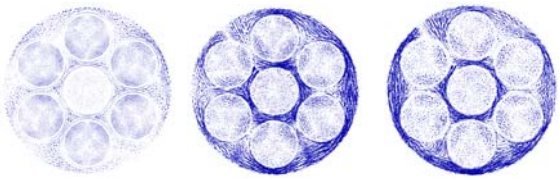

(a) (b) (c)

Fig.6 Velocity vectors in *X*-*Z* plane ($\dot{m}_h$ =1.5 m^3/h). (a) Model A; (b) Model B; (c) Model C

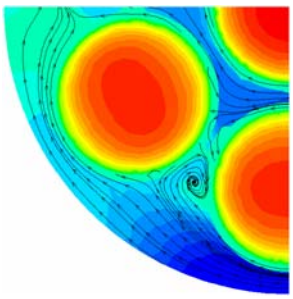

Fig.7 Temperature distribution and path lines of model B (in part of *X*-*Z* plane, $\dot{m}_h$ = 1.5 m^3/h)

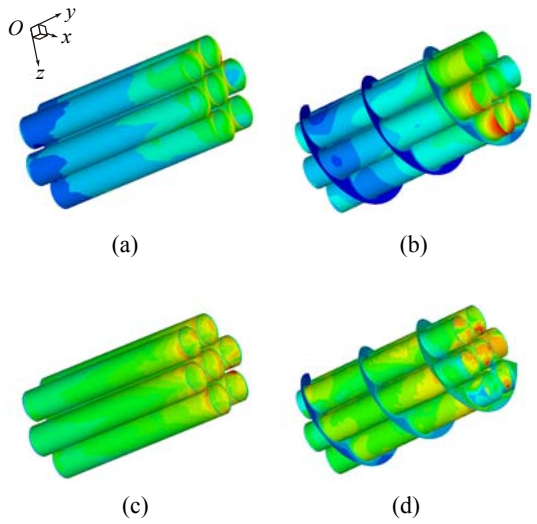

Fig.8 Distribution of the temperature and the surface heat transfer coefficient ($\dot{m}_h = 0.89\ m^3/h$). (a) Temperature, model A; (b) Temperature, model B; (c) Heat transfer coefficient, model A; (d) Heat transfer coefficient, model B

The frictional influences of three models are displayed in Figs.9 and 10. As the volumetric flow increased, the shell side pressure drop increased. Proper attention is required in that the shell side pressure drop of model C is less than that of model A in the same condition. The probable reason is that the tangential water intake of model C could avoid direct impact on the tube wall. Hence the hydraulic impact pressure is obviously reduced. As shown in Table 1, the pressure drop of model C is about 25% less than that of model B.

Fig.11 plots the heat transfer coefficient vs water Reynolds number. The higher the Reynolds number, the stronger is the turbulent flow generated. The heat transfer rate is enhanced correspondingly. In this evaluation model B exhibits the best heat transfer performance of the three models. Under the same water Reynolds number, the heat transfer coefficient of model B is about 4% higher than that of model C, especially with a big Reynolds number. In model A the heat transfer coefficient is about 4.2% to 10.28% lower compared to model B. Actually the difference between model A and model B of temperature (Table 1) is much more notable than that of the heat transfer coefficients. The reason is that the total area of seven tubes and helical baffle are considered as the heat transfer area (factor A) in models B and C, but only the tube-surface area is accounted for in model A. As shown in Eq.(9), the bigger the factor A, the less the heat transfer coefficient accordingly, which lessens the heat transfer coefficient difference between models A and B.

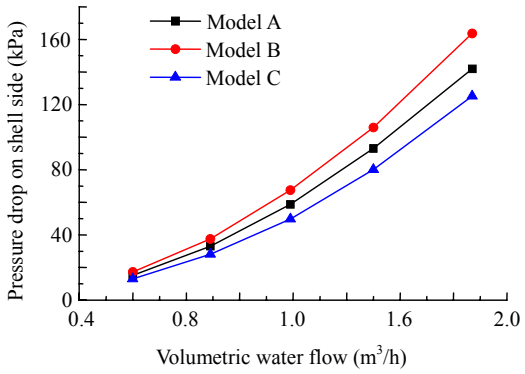

Fig.9 Pressure drop on shell side

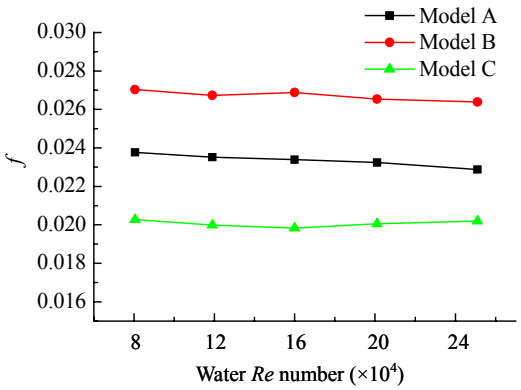

Fig.10 Friction factor vs *Re* number

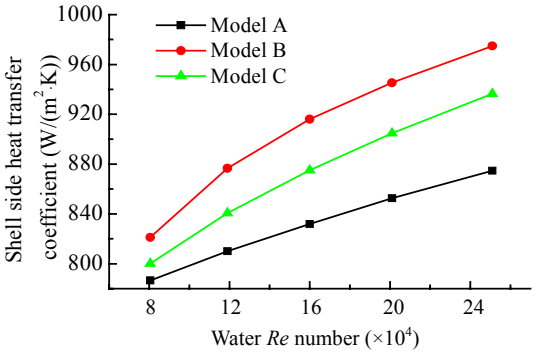

Fig.11 Shell side heat transfer coefficient vs *Re* number

CONCLUSION

The present study deals with a CFD analysis for the flow structures and temperature distributions of the EGR cooler. The numerical results contribute to discovering the inside flow and temperature field, and revealing the influence of the helical baffle and novel inlet geometry.

It is noticed that the temperature and heat transfer coefficient of the helical baffle are much lower than those of the tube wall. The primary benefit of the helical baffle is to lengthen the water flow path and to strengthen the swirl flow. The inlet angle influences the flow resistance significantly.

Using the same water Reynolds number, model B performs the best among the three models as far as heat transfer is concerned, and the differences grow significantly when the Reynolds number increases. In conclusion, we suggest that the improved structure, models B and C, are more effective in heat exchange performance than the traditional one.

The limitation of the present study resides in the fact that there is no experimental evidence. Further investigation, such as model fabrication, experimentation and comparative analysis will be executed in future research.

References

Dong, Q.W., Wang, Y.Q., Liu, M.S., 2008. Numerical and experimental investigation of shellside characteristics for ROD baffle heat exchanger. *Applied Thermal Engineering*, **28**(7):651-660. [doi:10.1016/j.applthermaleng.2007.06.038]

Eiamsa-ard, S., Promvonge, P., 2007. Heat transfer characteristics in a tube fitted with helical screw-tape with/without core-rod inserts. *International Communications in Heat and Mass Transfer*, **34**(2):176-185. [doi:10.1016/j.icheatmasstransfer.2006.10.006]

Grunenwald, B., Felber, S., Schmitz, A., Hetting, M., 2001. Laser Welding EGR Coolers—A New Process Technology for Exchanger Manufacturing. Vehicle Thermal Management Systems Conference and Exposition, Nashville, TN, USA.

Guo, Z.Y., Li, D.Y., Wang, B.X., 1998. A novel concept for convective heat transfer enhancement. *International Journal of Heat and Mass Transfer*, **41**(14):2221-2225. [doi:10.1016/S0017-9310(97)00272-X]

Jafari Nasr, M.R., Shafeghat, A., 2007. Fluid flow analysis and extension of rapid design algorithm for helical baffle heat exchangers. *Applied Thermal Engineering*, **28**(11-12):1324-1332. [doi:10.1016/j.applthermaleng.2007.10.021]

Launder, B., Spalding, D.B., 1972. Mathematical Models of Turbulence. Academic Press, London.

Lutcha, J., Nemcansky, J., 1990. Performance improvement of tubular heat exchangers by helical baffles. *Chemical Engineering Research and Design*, **68**(1):263-270.

Master, B., Chunangad, K., Pushpanathan, V., 2003. Fouling Mitigation Using Helixchanger Heat Exchangeres. Proceedings of the ECI Conference on Heat Exchanger Fouling and Cleaning: Fundamentals and Applications, Santa Fe, NM, p.317-322.

Pantow, E., Kern, J., Banzhaf, M., Lutz, R., Tillmann, A., 2001. Impact of US02 and Euro4 Emission Legislation on Power Train Cooling-challenges and Solution for Heavy Duty Trucks. Vehicle Thermal Management Systems Conference and Exposition, Nashville, TN, USA.

Peng, B., Wang, Q.W., Zhang, C., Xie, G.N., Luo, L.Q., Cheng, Q.Y., Zeng, M., 2007. An experimental study of shell-and-tube heat exchangers with continuous helical baffles. *Journal of Heat Transfer*, **129**(10):1425-1431.

Stehlík, P., Nemcansky, J., Kral, D., Swanson, L.W., 1994. Comparison of correction factors for shell-and-tube heat exchangers with segmental or helical baffles. *Heat Transfer Engineering*, **15**(1):55-65. [doi:10.1080/01457639408939818]

Stolz, A., Fleischer, K., Knecht, W., Nies, J., Strahle, R., 2001. Development of EGR Coolers for Truck and Passenger Car Application. Vehicle Thermal Management Systems Conference and Exposition, Nashville, TN, USA.